Electronic Supplementary Material (ESI) for Nanoscale.

Supplementary Information

Hollow Core-sheath nanocarbon sphere grown on carbonized silk fabric for self-supported and nonenzymatic glucose sensing

Wangdong Lu, Muqiang Jian, Qi Wang, Kailun Xia, Mingchao Zhang, Huimin Wang, Wenya He, Haojie Lu, and Yingying Zhang*

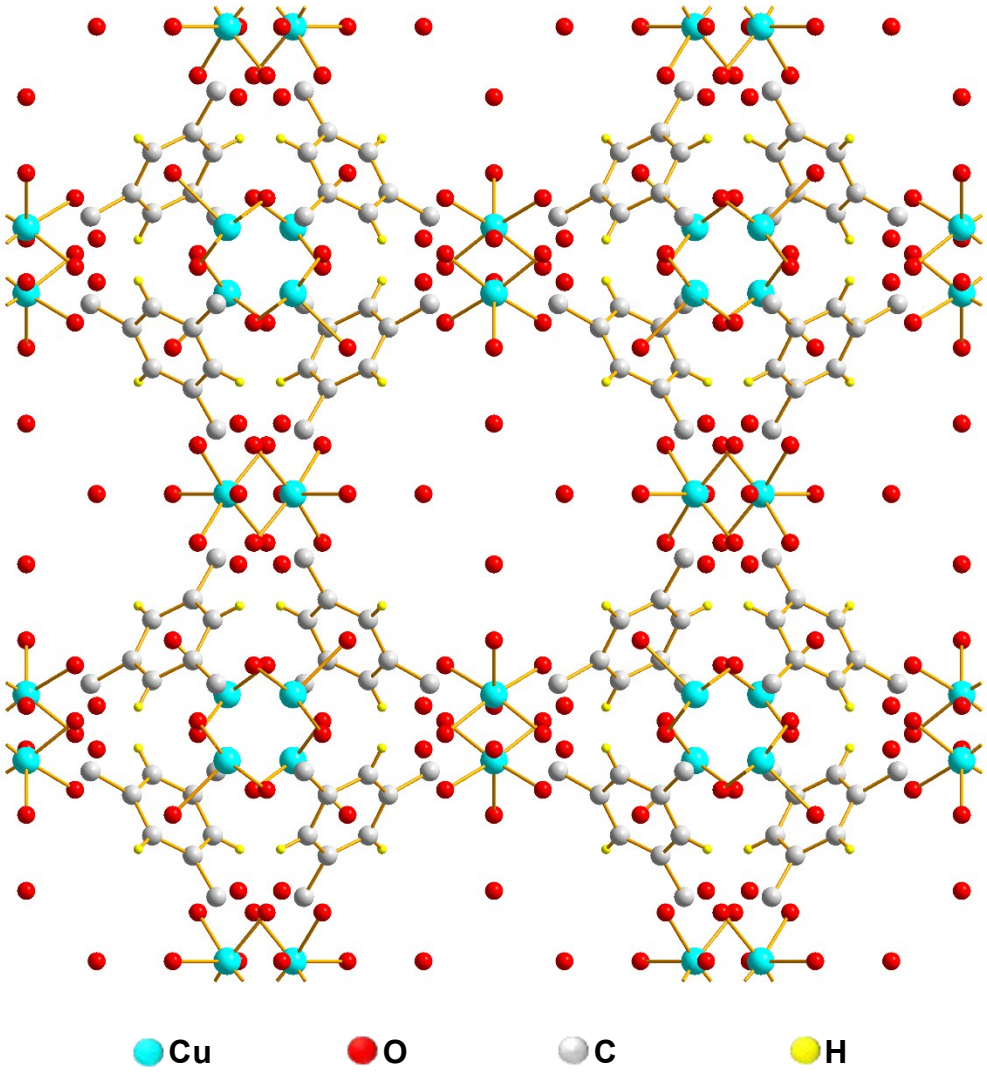

Figure S1. The crystal structure of HKUST-1.

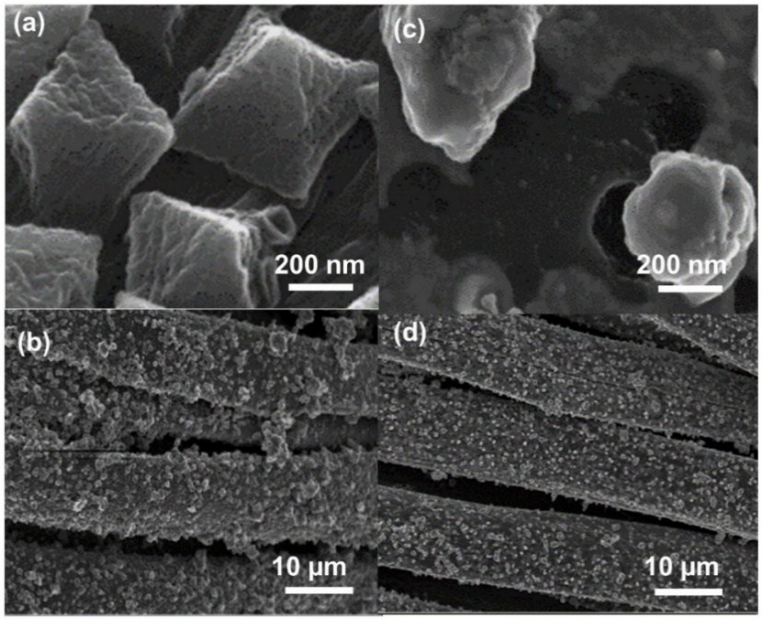

Figure S2. (a-d) SEM images of Cu-BTC on the silk fabric treated at different reaction temperature, 850°C (a, b) and1050°C (c, d).

Discussion about XPS spectra of Cu_2O NPs@CSs/CSF.

The element and surface electronic state of Cu_2O NPs@CSs/CSF were studied by XPS analysis (Figure S3). The high-resolution spectrum shows that the binding energies of Cu $2p_{1/2}$ and Cu $2p_{3/2}$ are located at 952.2 and 932.4 eV. However, the peak located at 932.4 eV cannot be directly attributed to Cu^+ since the Cu $2p_{3/2}$ binding energy peaks of metallic copper and Cu_2O are very close. Therefore, the two substances cannot be differentiated. However, according to the position of their LMM-2 Auger transition in XPS spectra, characteristic peaks of Cu and Cu_2O are assigned to 568 eV and 570 eV, respectively.[1, 2] From the surveyed XPS spectra (Figure S3a), a peak appears at about 570 eV, which demonstrates the existence of Cu_2O.

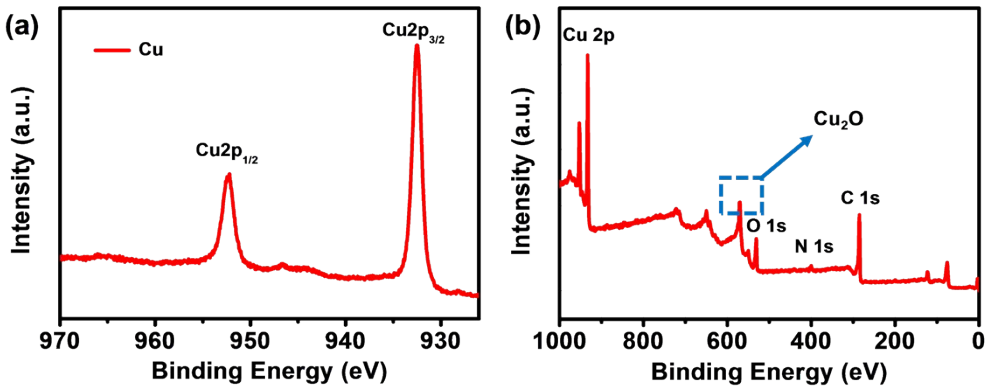

Figure S3. XPS spectra of Cu_2O NPs@CSs/CSF. (a) High-resolution spectrum of Cu. (b) Survey spectrum of Cu_2O NPs@CSs/CSF, indicating the presence of Cu_2O.

Discussion about EIS of Cu_2O NPs@CSs/CSF.

The EIS was implemented by CHI 760E electrochemical workstation with a three-electrode system. The EIS generally comprises a semicircular part and a linear part. The semicircular part at higher frequencies refers to the electron transfer limited process, and the diameter is attributable to the electron transfer resistance (Rct), which reflects the conductivity of composites. The linear part at lower frequencies is assigned to the diffusion process. From the Nyquist plot (Figure S4), the Cu_2O NPs@CSs/CSF electrode possesses a low resistance, indicating its good conductivity.

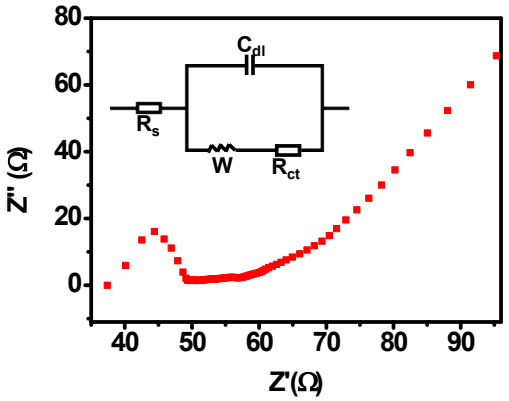

Figure S4. Nyquist plot of Cu_2O NPs@CSs/CSF electrode in 0.1M KCl electrolyte solution containing 0.01M $Fe(CN)_6^{3-/4-}$. Scan rate: 50mVs^{-1}.

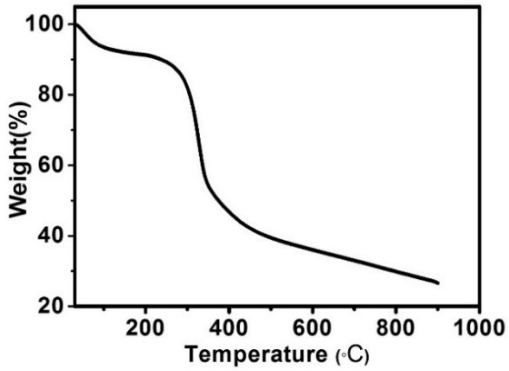

Figure S5. TGA curve of HKUST-1 in N_2 atmosphere.

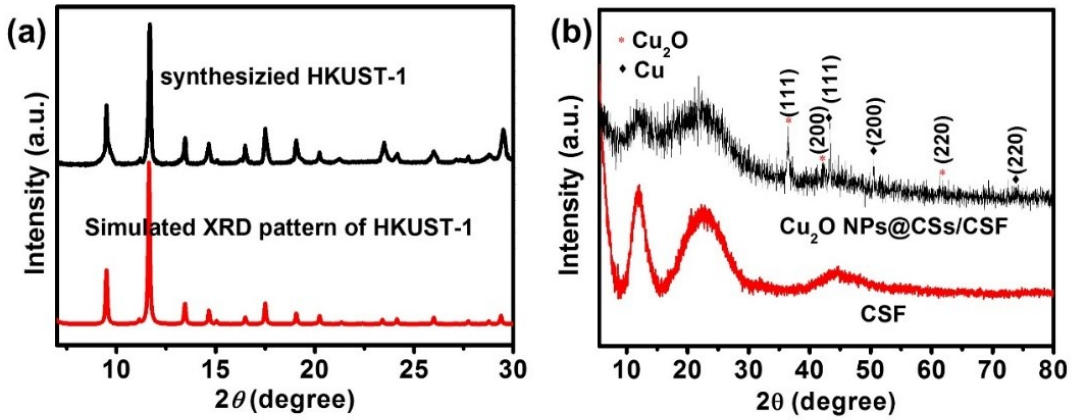

Figure S6. (a) XRD patterns of HKUST-1. (b) XRD patterns of CSF and Cu_2O NPs@CSs/CSF.

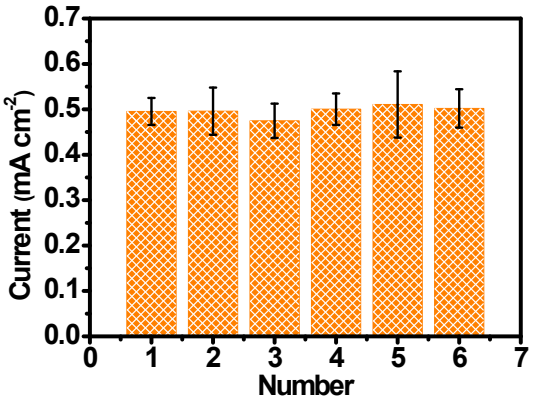

Figure S7. Amperometric response of different Cu_2O NPs@CSs/CS electrodes to the successive injection of 500 μM glucose after bending test.

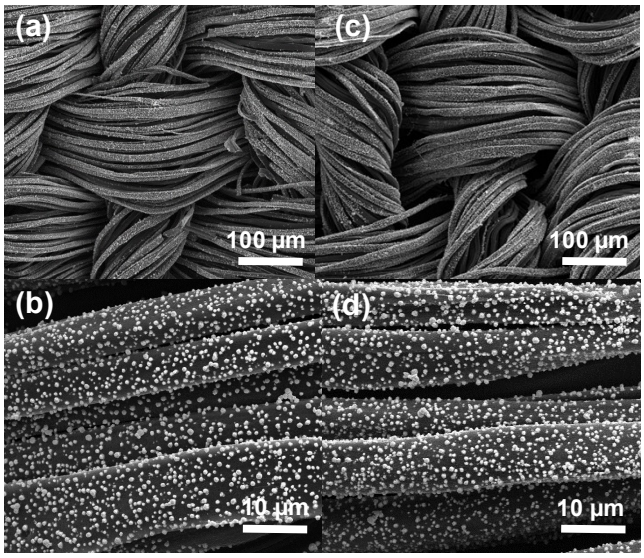

Figure S8. SEM images of Cu_2O NPs@CSs/CSF before bending and after bending. (a-b) SEM images of Cu_2O NPs@CSs/CSF before bending. (c-d) SEM images of Cu_2O NPs@CSs/CSF after bending.

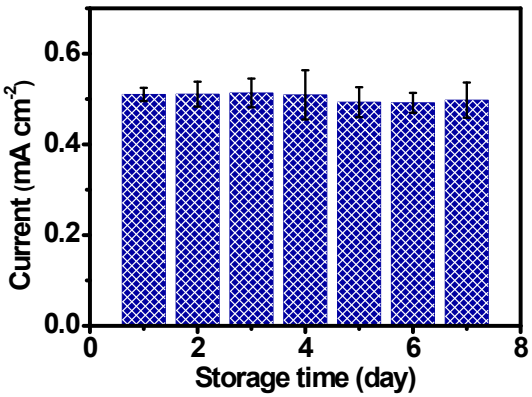

Figure S9. Amperometric response of different Cu_2O NPs@CSs/CS electrodes to the successive injection of 500 μM glucose for the long term stability measurement.

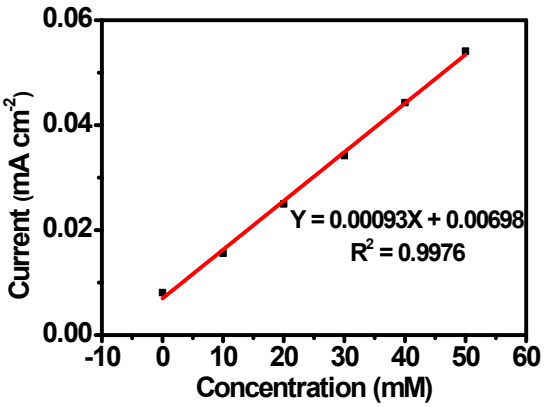

Figure S10. Glucose tests in serum based on standard addition method for the Cu_2O NPs@CSs/CSF Electrode.

References

1. T. Ghodselahi, M. A. Vesaghi, A. Shafiekhani, A. Baghizadeh, M. Lameii, *Appl Surf Sci.* **2008**, 255, 2730.
2. Dong, H. Zhong, T. Kou, J. Frenzel, G. Eggeler, Z. Zhang, *ACS Appl. Mater. Inter*. 2015, 7, 20215.